

# Visual detection of regional brain hypometabolism in cognitively impaired patients is independent of positron emission tomography-magnetic resonance attenuation correction method

## ABSTRACT

Fluorodeoxyglucose (FDG) positron emission tomography-magnetic resonance (PET/MR) is useful for the evaluation of cognitively-impaired patients. This study aims to assess two different attenuation correction (AC) methods (Dixon-MR and atlas-based) versus index-standard computed tomography (CT) AC for the visual interpretation of regional hypometabolism in patients with cognitive impairment. Two board-certified nuclear medicine physicians blindly scored brain region FDG hypometabolism as normal versus hypometabolic using two-dimensional (2D) and 3D FDG PET/MR images generated by MIM software. Regions were quantitatively assessed as normal versus mildly, moderately, or severely hypometabolic. Hypometabolism scores obtained using the different methods of AC were compared, and interreader, as well as intra-reader agreement, was assessed. Regional hypometabolism versus normal metabolism was correctly classified in 16 patients on atlas-based and Dixon-based AC map PET reconstructions (vs. CT reference AC) for 94% (90%–96% confidence interval [CI]) and 93% (89%–96% CI) of scored regions, respectively. The averaged sensitivity/specificity for detection of any regional hypometabolism was 95%/94% ( $P = 0.669$ ) and 90%/91% ( $P = 0.937$ ) for atlas-based and Dixon-based AC maps. Interreader agreement for detection of regional hypometabolism was high, with similar outcome assessments when using atlas- and Dixon-corrected PET data in 93% ( $\kappa = 0.82$ ) and 93% ( $\kappa = 0.84$ ) of regions, respectively. Intrareader agreement for detection of regional hypometabolism was high, with concordant outcome assessments when using atlas- and Dixon-corrected data in 93%/92% ( $\kappa = 0.79$ ) and 92%/93% ( $\kappa = 0.78$ ). Despite the quantitative advantages of atlas-based AC in brain PET/MR, routine clinical Dixon AC yields comparable visual ratings of regional hypometabolism in the evaluation of cognitively impaired patients undergoing brain PET/MR and is similar in performance to CT-based AC. Therefore, Dixon AC is acceptable for the routine clinical evaluation of dementia syndromes.

**Keywords:** Attenuation correction, brain, dementia, Dixon, positron emission tomography-magnetic resonance

## INTRODUCTION

Fluorodeoxyglucose (FDG) positron emission tomography-magnetic resonance (PET/MR) is a new modality that offers potential advantages over PET/computed tomography (CT) in the evaluation of cognitively impaired patients. The increased tissue contrast of multiple complex MR sequences compared to CT provides a significantly greater amount of diagnostic information, and hybrid PET/MR scanners allow for PET and MR to be obtained in a single, convenient session, with many systems offering simultaneous imaging capabilities. Motion-correction functionality offers the potential to

**ANA M. FRANCESCHI<sup>1</sup>, VALENTINO ABBALLE<sup>1</sup>, ROY A. RAAD<sup>1</sup>, AARON NELSON<sup>2</sup>, KIMBERLY JACKSON<sup>1</sup>, JAMES BABB<sup>1</sup>, THOMAS VAHLE<sup>3</sup>, MATTHIAS FENCHEL<sup>3</sup>, YIQIANG ZHAN<sup>4</sup>, GERARDO HERMOSILLO VALADEZ<sup>4</sup>, TIMOTHY M. SHEPHERD<sup>1,5</sup>, KENT P. FRIEDMAN<sup>1</sup>**

<sup>1</sup>Department of Radiology, New York University Medical Center,


<sup>2</sup>Center for Advanced Imaging Innovation and Research, New York, NY, <sup>3</sup>MIM Software Inc., Cleveland, OH, <sup>4</sup>Siemens Medical Solutions, Malvern, PA, USA, <sup>5</sup>Siemens Healthcare GmbH, Erlangen, Germany

**Address for correspondence:** Dr. Ana M. Franceschi, 660 First Avenue, 2<sup>nd</sup> Floor, New York, NY 10016, USA. E-mail: ana.franceschi@nyumc.org

This is an open access journal, and articles are distributed under the terms of the Creative Commons Attribution-NonCommercial-ShareAlike 4.0 License, which allows others to remix, tweak, and build upon the work non-commercially, as long as appropriate credit is given and the new creations are licensed under the identical terms.

**For reprints contact:** reprints@medknow.com

**How to cite this article:** Franceschi AM, Abballe V, Raad RA, Nelson A, Jackson K, Babb J, *et al.* Visual detection of regional brain hypometabolism in cognitively impaired patients is independent of positron emission tomography-magnetic resonance attenuation correction method. *World J Nucl Med* 2018;17:188-94.

Access this article online	
<b>Website:</b> www.wjnm.org	<b>Quick Response Code</b> 
<b>DOI:</b> 10.4103/wjnm.WJNM_61_17	

improve PET image quality, and radiation exposure is reduced compared to PET/CT. PET/MR scans also encourage collaborative reading sessions between nuclear medicine physicians and neuroradiologists, which may improve the quality of image interpretation, particularly for complex cases and patients with multiple comorbidities.

Despite the above advantages of PET/MR over PET/CT for the evaluation of cognitive impairment, many recent studies have demonstrated that there are significant quantitative errors in estimates of brain metabolic activity associated with the first generation of PET/MR scanners.<sup>[1-3]</sup> The primary source of this error is the lack of bone segmentation on anatomical attenuation maps generated by MR sequences obtained during PET/MR. The earliest versions of clinical scanners offered Dixon-based tissue segmentation for attenuation correction (AC) which classified air, soft tissues and fat; but had no accurate method to measure density or location of bone. With this type of MRAC, whole-brain activity has been reported to be underestimated by 6.4%, and regional activity can be underestimated by up to 12%.<sup>[4]</sup> Individual voxels may be even more severely affected.<sup>[5,6]</sup>

Much work is underway to improve the means by which PET attenuation is calculated on PET/MR scanners. Methods employed include ultrashort echo time sequences (UTE) and zero-echo time sequences (ZTE) that provide estimates of bone location,<sup>[7-9]</sup> atlas-based techniques,<sup>[10-12]</sup> and hybrid methods combining the patient's own MR sequences (such as MPRAGE) with UTE-based estimates of bone.<sup>[13-16]</sup> Even more sophisticated systems including a combination of UTE + R2\* mapping<sup>[13]</sup> have the potential to not only localize but also estimate the density of bone. Other techniques under development rely on time-of-flight PET emission data to estimate the location of bone.<sup>[17]</sup>

It remains to be seen exactly which methods of MRAC will be applied in Food and Drug Administration (FDA)-approved clinical systems in the coming years, and at what time. It is likely that PET/MR systems at many institutions will still in the coming years predominantly employ MRAC techniques that do not account for bone, and there is a need to understand the clinical impact of Dixon-based MRAC on interpretation of brain scans in cognitively impaired patients, that represent a large percentage of referrals for clinical brain PET/MR at our institution (and likely others).

This study employs the patient's own CT images (derived from same-day PET/CT) as a reference standard to assess the impact, if any, of three different AC methods (CT-based, Dixon-based, and a prototype atlas-based AC method) on the

blinded visual interpretation of regional hypometabolism in patients with cognitive impairment evaluated by FDG PET/MR. Our study focused not only on identification of regional hypometabolism but semi-quantitative visual scoring of the severity of hypometabolism as well.

## MATERIALS AND METHODS

### Patient selection

This HIPAA-compliant study received local institutional review board IRB approval. Patients referred for clinically indicated brain FDG PET/CT were recruited for a research PET/magnetic resonance imaging (MRI) examination from October 2012 to October 2013. All patients provided written informed consent for the study – surrogate consent was obtained for patients unable to consent as per IRB guidelines. Sixteen consecutively enrolled patients with clinically suspected neurodegenerative disorders underwent brain FDG PET/CT immediately followed by a brain PET/MRI.

### Image acquisition

#### Positron emission tomography/magnetic resonance

All patients fasted for a minimum of 4 h before imaging. Insulin was withheld 6 h before imaging, and blood glucose concentration was verified to be <200 mg/dL. All patients received a 10-mCi dose of FDG. For 45 min after the injection, patients were instructed to sit quietly in a dimly lit room. Patients were asked to void before imaging. PET/CT images of the subjects' heads were acquired with a Biograph mCT system (Siemens Healthcare, Erlangen, Germany). The CT acquisition parameters were as follows: 120 kVp, 300 mA, 3.0 mm slice width, 1.5 mm slice interval, 30-cm transaxial field-of-view FOV, 512 × 512 image matrix, B40f convolution kernel. The PET acquisition parameters were as follows: 15-min single-bed acquisition of the brain from the skull vertex to the foramen magnum, 400-mm transaxial FOV, 221-mm axial FOV, 512 × 512 transaxial matrix, and 3-mm Gaussian postreconstruction image filter. PET images were reconstructed with CT for AC with the attenuation-weighting ordered subsets expectation-maximization 3D algorithm (OSEM3D) at 6 iterations and 12 subsets. The transaxial voxel dimensions were 1.02 × 1.02 mm with a thickness of 1.5 mm.

#### Positron emission tomography/magnetic resonance imaging

PET/MRI studies were performed using a Biograph mMR scanner (Siemens Healthcare, Erlangen, Germany). The PET detector is composed of lutetium oxyorthosilicate scintillation crystals attached to avalanche photodiodes replacing typical photomultiplier tubes used in PET/CT. Each block detector consists of 64 crystal elements, and each

crystal measures 4 mm × 4 mm × 20 mm. In each ring are 56 block detectors, and a total of 64 detector element rings are arranged along the z-axis. The MRI unit is equipped with a 3-T magnet.

PET and MRI data were acquired simultaneously. From the skull vertex to the foramen magnum, a dual-echo T1-weighted gradient-recalled echo sequence was performed to acquire the MRI attenuation-correction map based on a Dixon segmentation (air, fat, soft tissue, and lungs). Afterward, routine diagnostic MRI sequences were performed while PET data were simultaneously acquired for a total of 45 min. The PET data were reconstructed with an iterative 3D ordinary Poisson ordered subsets expectation–maximization algorithm at 3 iterations and 21 subsets and with a 4-mm Gaussian postreconstruction image filter. The PET image matrix size was 344 mm × 344 mm × 127 mm. The transaxial voxel dimensions were 1.04 mm × 1.04 mm with a thickness of 2.03 mm.

### Image analysis

MIMneuro version 6.1 (MIM Software, Inc., Cleveland, Ohio, USA) was used to perform the visual comparative analysis of PET data obtained from PET/CT and PET/MRI. This is a FDA-approved image processing and viewing package used clinically at our medical center. Images were spatially normalized to a standard brain template using a process of image translation, rotation, and scaling followed by an iterative landmark matching and thin-plate deformable registration technique. 3D stereotactic surface projections were created for both PET/CT- and PET/MRI-derived PET data.

A manufacturer-provided non-product offline reconstruction tool was used to reconstruct PET data obtained from PET/MR with AC based on the patient's own CT images, a Dixon-MR-derived AC map and a prototype atlas-based AC map that combined Dixon-MR with an estimation of bony skull structures [Figure 1].<sup>[4]</sup>

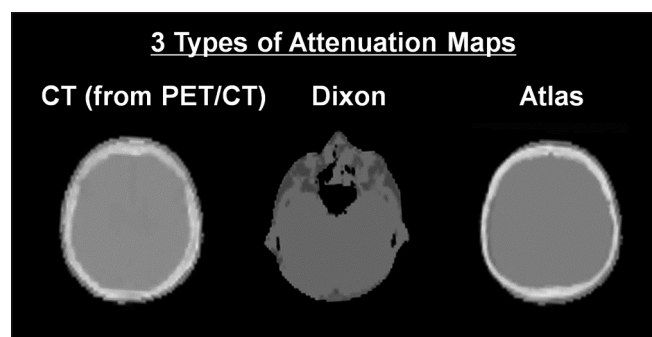


**Figure 1: Example of two different attenuation correction maps (Dixon-MR-based or atlas-based) utilized in positron emission tomography/magnetic resonance imaging reconstruction compared to the computed tomography reference standard**

Two nuclear medicine physicians with experience in PET interpretation (12 years' reader #1; 3 years' reader #2) interpreted the PET portion of all PET/MRI images and blindly scored 10 brain regions (frontal, temporal, parietal, occipital, and precuneus on each side) as normal versus hypometabolic using two-dimensional (2D) and 3D images generated by MIM software. Normal regions were scored as 0, whereas abnormal regions were scored as mildly, moderately, or severely hypometabolic (score of 1, 2, or 3, respectively).

### Statistical analysis

The hypometabolism scores obtained using the different methods of AC were compared, and inter- and intra-reader agreement was assessed. All statistical tests were conducted at the two-sided 5% significance level using SAS 9.3 (SAS Institute, Cary, NC, USA).

### RESULTS

Regional hypometabolism versus normal metabolism was correctly classified (accuracy) for 160 regions in 16 patients by two readers on atlas-based and Dixon-based AC map PET reconstructions (vs. CT reference AC) for 94% (90%–96% confidence interval [CI]) and 93% (89%–96% CI) of all regions [Figures 2 and 3 for representative 3D surface projections].

The averaged sensitivity/specificity for detection of any regional hypometabolism was 95%/94% ( $P = 0.669$ ) and 90%/91% ( $P = 0.937$ ) for atlas-based and Dixon-based AC maps, respectively, compared to the reference standard CT images [Table 1]. The mean absolute error of regional hypometabolism scores for atlas-based and Dixon-based PET reconstructions (versus CT) was  $0.25 \pm 0.44$  and  $0.21 \pm 0.42$ , respectively [Table 2].

Interreader agreement for detection of regional hypometabolism was high, with similar outcome assessments when using atlas- and Dixon-corrected PET data in 93% and 93% of scored regions, respectively [Table 3]. The simple kappa coefficient to assess reader agreement in terms of hypometabolism versus normal regions was 0.82 for atlas- and 0.84 for Dixon-based AC. The weighted kappa coefficient to assess reader agreement in terms of the hypometabolism score was 0.75 for atlas- and 0.77 for Dixon-based AC. All kappa values imply substantial interreader agreement.

Intrareader agreement for detection of regional hypometabolism was high, with concordant outcome assessments when using the same method (atlas- and Dixon-corrected PET data) to evaluate the same region of the same patient on two separate occasions in 93%/92% (reader 1/reader 2) and 92%/93% (reader 1/reader 2) of scored

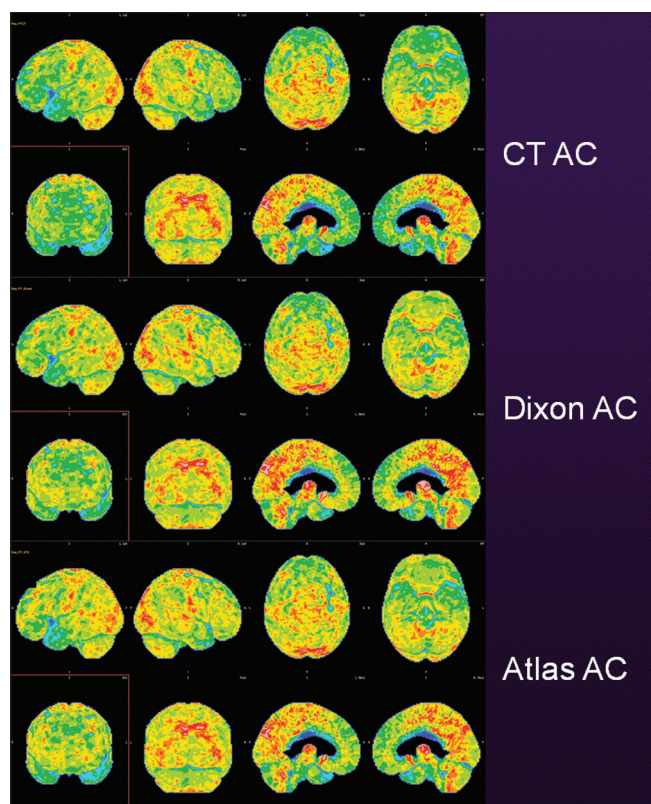


Figure 2: Case example, fused computed tomography from positron emission tomography/computed tomography “gold standard” attenuation correction (top), Dixon-MR-based (middle) and atlas-based attenuation correction (bottom) in a patient with moderate hypometabolism in the frontal, parietal, and temporal lobes bilaterally: AD versus FTD pattern

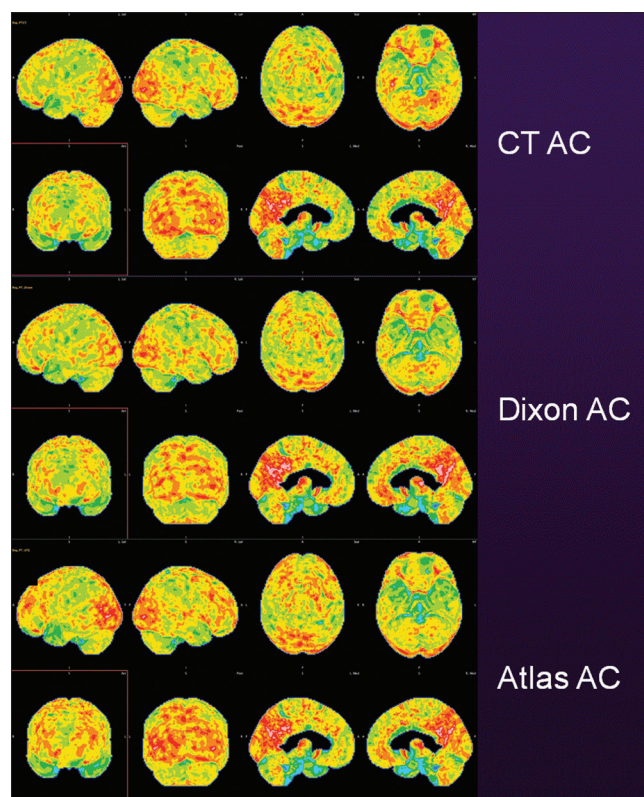


Figure 3: Case example, fused computed tomography from positron emission tomography/computed tomography “gold standard” attenuation correction (top), Dixon-MR-based (middle) and atlas-based attenuation correction (bottom) in a patient with mild hypometabolism in the parietal and temporal lobes bilaterally: AD pattern

regions, respectively [Table 4]. The simple kappa coefficient to assess intrareader agreement in terms of hypometabolism versus normal regions was 0.79 for atlas- and 0.78 for Dixon-based AC. The linear weighted kappa coefficient to assess intrareader agreement in terms of the hypometabolism score was 0.79 for atlas- and 0.83 for Dixon- based AC. All kappa values implied substantial intrareader agreement.

## DISCUSSION

This study addresses the potential clinical diagnostic impact of AC errors in brain FDG PET/MR images reconstructed using Dixon-based AC techniques and evaluates the performance of a newer atlas-based algorithm. Our study is first an attempt to further explore and address concerns among PET/MR users that have suggested that Dixon-based AC is suboptimal for high-quality clinical PET/MR in patients with dementia. Second, we evaluated the diagnostic performance of a newer, increasingly quantitatively accurate atlas-based technique to determine if the additional processing time required by this method is helpful and/or necessary for all cognitively impaired patients being evaluated in a busy clinical practice.

Our main finding is that in cognitively impaired patients undergoing clinical brain PET/MR, there is no significant performance difference between the gold standard CT-based, Dixon-based and atlas-based AC techniques in the visual identification of hypometabolic regions considered critical for the identification and characterization of neurodegenerative disorders in patients with cognitive impairment. Of note, the vast majority of patients seen in our department were found to have either imaging findings suggestive of Alzheimer’s dementia, Lewy body dementia, frontotemporal dementia, or variants of primary progressive aphasia. These conditions are diagnosed by identifying patterns of hypometabolism in the temporal, parietal, frontal, and occipital lobes as well as in the precuneus. In our study, Dixon-based AC identified pathology in these regions with an overall performance that was statistically no different than the same PET data reconstructed using the subject’s own fused and processed CT images, as would have been done had the patient only been evaluated by PET/CT. Furthermore, although possibly preferred by physicians once widely available, quantitatively superior atlas-based techniques<sup>[4]</sup> do not seem to result in improvements in clinical interpretation of hypometabolic brain regions.

**Table 1: The estimate of sensitivity and specificity for the detection of any abnormality of each method relative to computed tomography, the lower and upper limits of a 95% confidence for the specificity and sensitivity of each method and the P value from GEE to compare methods in terms of specificity and sensitivity**

	Reader	Atlas			Dixon			P
		Estimate	Lower	Upper	Estimate	Lower	Upper	
Sensitivity	1	98.1% (104/106)	0.88	1.00	95.3% (101/106)	0.89	0.98	0.324
	2	92.1% (105/114)	0.83	0.96	93.0% (106/114)	0.85	0.97	0.759
	Both	95.0% (209/220)	0.89	0.98	94.1% (207/220)	0.89	0.97	0.669
Specificity	1	90.9% (40/44)	0.77	0.97	90.9% (40/44)	0.77	0.97	1.000
	2	88.9% (32/36)	0.72	0.96	91.7% (33/36)	0.72	0.98	0.659
	Both	90.0% (72/80)	0.80	0.95	91.3% (73/80)	0.75	0.97	0.937

GEE: Generalized estimating equation

**Table 2: The mean±standard deviation of the errors in the hypometabolism scores of each method relative to computed tomography and P values from the Wilcoxon signed-rank test to compare methods in terms of the errors**

Reader	Atlas	Dixon	P
1	0.17±0.37	0.17±0.37	0.929
2	0.33±0.49	0.26±0.46	0.124
Both	0.25±0.44	0.21±0.42	0.136

**Table 3: Interreader agreement**

Outcome	Atlas	Dixon
Normal versus abnormal region	92.7% (139/150)	93.3% (140/150)
Score of regional hypometabolism	75.3% (113/150)	73.3% (110/150)

The fact that the Dixon-based technique performed well when it comes to visual identification of hypometabolic brain regions is not terribly surprising when one looks at the distribution of the undercorrection errors present in AC maps that do not account for bone.<sup>[4-6]</sup> Careful inspection of the undercorrection bias maps generally demonstrates a relatively smooth, circumferential pattern where outer surfaces of the brain are underestimated in a relatively homogeneous symmetric pattern, with decreasing undercorrection present as one moves deeper into the brain. Given that neurodegenerative disorders are generally diagnosed on FDG PET by looking at the outer surface of the cerebrum and in particular comparing to the usually spared occipital lobes, the generalized underestimation around the periphery of the brain has the effect of relatively uniformly decreasing the standardized uptake value (SUV) values throughout the cerebrum without negatively impacting relative differences. The only exception to this concept may be at the orbitofrontal and polar regions of the frontal lobes,<sup>[4]</sup> but this region is not particularly critical in the identification of most neurodegenerative diseases. More specifically, we hypothesize that patients with frontotemporal dementia typically have an injury pattern that involves a large enough portion of the frontal lobes such that higher errors in the inferior (orbitofrontal) region do not negatively impact image

interpretation. Furthermore, known errors at the skull-base and cerebellum similarly do not impact identification of common neurodegenerative diseases. Although some sites may rely on the cerebellum for image normalization in processing or interpretation methodologies, in our experience, there is too much variability in relative cerebellar activity (possibly due to medications or other effects) in patients undergoing any type of brain FDG PET imaging, be it PET/CT or PET/MR, to rely on this region for identification of cerebral hypometabolism. Future studies similar to ours in patients with parkinsonian syndromes and other conditions that may preferentially impact deeper brain structures and the cerebellum should be encouraged.

This study results support our hypothesis that cognitively impaired patients can undergo FDG brain PET/MR using Dixon-based AC and benefit from accurate interpretations similar to conventional PET/CT. However, some caveats should be considered before applying our results to all types of brain PET/MR. First, our patient population consists predominantly of patients with moderate-to-severe symptoms, with a fewer number of patients presenting to our department with mild cognitive impairment. Although we believe our study contained enough “normal” brain regions to reasonably evaluate the ability of Dixon- and atlas-based AC to distinguish between “normal” and “mild hypometabolism” compared to CTAC, on a per-patient basis, we did not evaluate subjects with normal findings throughout every single brain region, and thus, we feel that further studies should be performed to determine if there are any performance differences between the various types of MRAC for departments that are scanning a large number of patients with mild symptoms, be it for research or otherwise, within a large health-care system. A second caveat is that these results may not be uniformly applicable to all patients undergoing evaluation for epilepsy, brain tumors or studies in which other radiopharmaceuticals are employed. It is worth noting that preliminary results have suggested that Dixon-based AC may also be sufficient for identification of amyloid-positivity in patients scanned with florbetapir, with Su *et al.* reporting 12 of 40 subjects classified

**Table 4: Intrareader agreement**

Outcome	Atlas		Dixon	
	Reader 1	Reader 2	Reader 1	Reader 2
Normal versus abnormal region	92.5% (111/120)	91.7% (110/120)	91.7% (110/120)	92.5% (111/120)
Score of regional hypometabolism	81.7% (98/120)	71.7% (86/120)	83.3% (100/120)	79.2% (95/120)

as amyloid positive using both Dixon- and CT-based MRAC for correction of PET data obtained on a PET/MR scanner.<sup>[3]</sup>

There are limited published data addressing the visual clinical interpretation of brain FDG PET data obtained from PET/MR, with most studies focusing strictly on quantitative aspects and very few comparing PET data obtained only from a PET/MR scanner with the only difference in the comparisons being the method of AC. One recent paper examined patients in a fashion similar to ours, studying 13 patients of which 9 were classified as normal using CT-based AC while 3 patients were diagnosed with AD, one with FTLD, and one with hypometabolism but no specific diagnosis.<sup>[16]</sup> The authors compared four AC techniques including Dixon; a CT obtained from PET/CT, a “pseudo-CT” derived from T1 MPRAGE images, and a fourth technique which extracted bone information from UTE sequences and superimposed it upon soft tissue information from Dixon-based data. There was no significant difference in the number of hypometabolic regions identified using all four techniques. The higher number of “normal” participants in this study may preliminarily suggest that Dixon-based AC can accurately differentiate between normal and mild hypometabolism among larger patient populations with mild symptoms, as no significant false-positives were observed. Of note, our study further refined this type of analysis of visual reading interpretation by requiring readers to visually rate degrees of hypometabolism (mild, moderate, and severe). The fact that most visual scores were within one degree of variability (mild vs. moderate and moderate vs. severe) further suggests that visual interpretation is relatively accurate even with the known quantitative errors of Dixon-MR. Inter- and intra-reader agreement was high (greater than 92%) for the distinction between abnormal and normal regions, thus both reconstruction techniques (Dixon and atlas) appear to be equally robust, and neither technique demonstrated any features that impacted reader performance. Slightly lower interreader (75% for atlas, 73% for Dixon) and intrareader (72%–83%) agreements for specific regional hypometabolism scores highlight inherent challenges in visual interpretation of quantitative data but confirms our suspicions that observed mild variability in interpretation is more due to reader performance and not the specific reconstruction techniques, and it should be emphasized that this phenomenon exists in routine clinical practice. It is worth noting that the degree of hypometabolism

(mild vs. moderate and moderate vs. severe) is less important than the pattern of hypometabolism distribution in the diagnosis of dementia syndromes.

Finally, the UTE-based technique tested in the study by Werner *et al.* suggests that newer UTE/ZTE techniques may similarly offer no meaningful clinical advantage over Dixon with respect to visual interpretation in this particular clinical scenario, but further studies are certainly warranted, and improved quantification may be of value in other clinical scenarios.<sup>[16]</sup>

## CONCLUSION

Despite the more accurate FDG SUV quantification realized with implementation of CT-based and atlas-based AC in brain PET/MR compared to Dixon AC, there were no measurable differences between the three AC methods with respect to visual identification of regional hypometabolism in the evaluation of cognitively impaired patients. PET/MR users that currently only have Dixon-based MRAC installed on their systems can rest assured that FDG PET image quality is acceptable in the evaluation of patients with cognitive impairment. As atlas-based techniques or newer UTE/ZTE methods become more widely available, users may wish to switch to these methodologies to achieve improved quantification, though our study reemphasizes that clinical reporting using Dixon-based MRAC represents the high quality standard of care.

## Financial support and sponsorship

Nil.

## Conflicts of interest

There are no conflicts of interest.

## REFERENCES

1. Aasheim LB, Karlberg A, Goa PE, Håberg A, Sørhaug S, Fagerli UM, *et al.* PET/MR brain imaging: Evaluation of clinical UTE-based attenuation correction. *Eur J Nucl Med Mol Imaging* 2015;42:1439-46.
2. Bailey DL, Pichler BJ, Gückel B, Barthel H, Beer AJ, Botnar R, *et al.* Combined PET/MRI: From Status Quo to Status Go. Summary Report of the Fifth International Workshop on PET/MR Imaging; February 15-19, 2016; Tübingen, Germany. *Mol Imaging Biol* 2016;18:637-50.
3. Su Y, Rubin BB, McConathy J, Laforest R, Qi J, Sharma A, *et al.* Impact of MR-based attenuation correction on neurologic PET studies. *J Nucl Med* 2016;57:913-7.
4. Koesters T, Friedman KP, Fenchel M, Zhan Y, Hermosillo G,

- Babb J, *et al.* Dixon sequence with superimposed model-based bone compartment provides highly accurate PET/MR attenuation correction of the brain. *J Nucl Med* 2016;57:918-24.
5. Andersen FL, Ladefoged CN, Beyer T, Keller SH, Hansen AE, Højgaard L, *et al.* Combined PET/MR imaging in neurology: MR-based attenuation correction implies a strong spatial bias when ignoring bone. *Neuroimage* 2014;84:206-16.
  6. Catana C, van der Kouwe A, Benner T, Michel CJ, Hamm M, Fenchel M, *et al.* Toward implementing an MRI-based PET attenuation-correction method for neurologic studies on the MR-PET brain prototype. *J Nucl Med* 2010;51:1431-8.
  7. Ladefoged CN, Benoit D, Law I, Holm S, Kjær A, Højgaard L, *et al.* Region specific optimization of continuous linear attenuation coefficients based on UTE (RESOLUTE): Application to PET/MR brain imaging. *Phys Med Biol* 2015;60:8047-65.
  8. Burgos N, Cardoso MJ, Thielemans K, Modat M, Dickson J, Schott JM, *et al.* Multi-contrast attenuation map synthesis for PET/MR scanners: Assessment on FDG and florbetapir PET tracers. *Eur J Nucl Med Mol Imaging* 2015;42:1447-58.
  9. Sekine T, Ter Voert EE, Warnock G, Buck A, Huellner M, Veit-Haibach P, *et al.* Clinical evaluation of zero-echo-time attenuation correction for brain 18F-FDG PET/MRI: Comparison with atlas attenuation correction. *J Nucl Med* 2016;57:1927-32.
  10. Sekine T, Buck A, Delso G, Ter Voert EE, Huellner M, Veit-Haibach P, *et al.* Evaluation of atlas-based attenuation correction for integrated PET/MR in human brain: Application of a head atlas and comparison to true CT-based attenuation correction. *J Nucl Med* 2016;57:215-20.
  11. Sekine T, Burgos N, Warnock G, Huellner M, Buck A, Ter Voert EE, *et al.* Multi-atlas-based attenuation correction for brain 18F-FDG PET imaging using a time-of-flight PET/MR scanner: Comparison with clinical single-atlas-and CT-based attenuation correction. *J Nucl Med* 2016;57:1258-64.
  12. Chen KT, Izquierdo-Garcia D, Poynton CB, Chonde DB, Catana C. On the accuracy and reproducibility of a novel probabilistic atlas-based generation for calculation of head attenuation maps on integrated PET/MR scanners. *Eur J Nucl Med Mol Imaging* 2017;44:398-407.
  13. Ladefoged C, Benoit D, Law I, Holm S, Højgaard L, Hansen AE, *et al.* PET/MR attenuation correction in brain imaging using a continuous bone signal derived from UTE. *EJNMMI Phys* 2015;2:A39.
  14. Wu Y, Yang W, Lu L, Lu Z, Zhong L, Huang M, *et al.* Prediction of CT substitutes from MR images based on local diffeomorphic mapping for brain PET attenuation correction. *J Nucl Med* 2016;57:1635-41.
  15. Torrado-Carvajal A, Herraiz JL, Alcaín E, Montemayor AS, Garcia-Cañamaque L, Hernandez-Tamames JA, *et al.* Fast patch-based pseudo-CT synthesis from T1-weighted MR images for PET/MR attenuation correction in brain studies. *J Nucl Med* 2016;57:136-43.
  16. Werner P, Rullmann M, Bresch A, Tiepolt S, Jochimsen T, Lobsien D, *et al.* Impact of attenuation correction on clinical [(18)F] FDG brain PET in combined PET/MRI. *EJNMMI Res* 2016;6:47.
  17. Mehranian A, Arabi H, Zaidi H. Quantitative analysis of MRI-guided attenuation correction techniques in time-of-flight brain PET/MRI. *Neuroimage* 2016;130:123-33.